A KS-type dehydrin and its related domains reduce Cu-promoted radical generation and the histidine residues contribute to the radical-reducing activities

Title

A KS-type dehydrin and its related domains reduce Cu-promoted radical generation and the His residues contribute to the radical-reducing activities

Authors

Masakazu Hara[1*], Mitsuru Kondo[2], Takanari Kato[1]

[1]Faculty of Agriculture, Shizuoka University,

836 Ohya, Shizuoka 422-8529, Japan

[2]Center for Instrumental Analysis, Shizuoka University,

836 Ohya, Shizuoka 422-8529, Japan

***Name and address for editorial correspondence**

Masakazu Hara

Faculty of Agriculture, Shizuoka University,

836 Ohya, Shizuoka 422-8529, Japan

Telephone & Fax number: +81-54-238-5134

E-mail address: amhara@ipc.shizuoka.ac.jp

E-mail addresses

Masakazu Hara, amhara@ipc.shizuoka.ac.jp; Mitsuru Kondo, scmkond@ipc.shizuoka.ac.jp; Takanari Kato, taisousuiren@hotmail.co.jp.

Running title

Inhibition of radical generation by dehydrin

One table, six figures, and three supplementary figures.

Total word count: 7393

Abstract

Dehydrin is a plant disordered protein whose functions are not yet totally understood. Here we report that a KS-type dehydrin can reduce the formation of radical oxygen species (ROS) from Cu. AtHIRD11, which is the *Arabidopsis* KS-type dehydrin, inhibited generations of hydrogen peroxide and hydroxyl radicals in the Cu-ascorbate system. The radical reducing activity of AtHIRD11 was stronger than those of radical silencing peptides such as glutathione and serum albumin. The addition of Cu^{2+} reduced the disordered state, decreased the trypsin susceptibility, and promoted the self-association of AtHIRD11. Domain analyses indicated that the five domains containing His showed ROS-reducing activities. His/Ala substitutions indicated that His is a crucial residue for reducing ROS generation. Using the 27 peptides which are related to the K_nS-type dehydrins of 14 plant species, we found that the strengths of ROS-reducing activities can be determined by two factors, i.e. the His contents and the length of the peptides. The degree of ROS-reducing activities of a dehydrin can be predicted using these indices.

Key words; Circular dichroism; dehydrin; disordered protein; heavy metal; histidine; reactive oxygen species

Introduction

Dehydrins (group 2 late embryogenesis abundant proteins) are plant proteins that are responsive to abiotic stresses such as drought, extreme temperature, and high salinity. Various plant species accumulate dehydrins during embryogenesis and stress responses. Studies on the conserved domains, expression, localization, conformational characteristics, and functions of dehydrins have been summarized (see reviews such as Close 1996; Svensson *et al*. 2002; Rorat 2006; Tunnacliffe and Wise, 2007; Battaglia *et al*. 2008; Hundertmark and Hincha 2008; Hara 2010; Eriksson and Harryson 2011). Dehydrins possess conserved K-segments (EKKGIMDKIKEKLPG or similar sequences), which are proposed to form an amphipathic helix (see reviews cited above). Other unique domains, i.e. a Y-segment (a typical sequence; DEYGNP) and S-segment (LHRSGSSSSSSSEDD or related sequences), frequently appear in dehydrin sequences. Using the three segments, dehydrins are conveniently classified by the following shorthand: SK_n, Y_nSK_n, Y_nK_n, K_nS, etc. Because dehydrins are composed of charged and polar amino acids, they are believed to have highly flexible structures (see reviews cited above). Dehydrins show boiling stability, abnormal mobility in electrophoresis, and high proteolytic sensitivity. Circular dichroism (CD), Fourier-transform infrared spectroscopy, and nuclear magnetic resonance indicated that dehydrins are intrinsically disordered proteins (Tompa, 2009).

Dehydrins are ubiquitously found in various subcellular compartments, including the cytoplasm, nucleus, plasma membrane, tonoplast, plastid, mitochondrion, endoplasmic reticulum, and plasmodesmata (see reviews cited above). Dehydrins have been detected mainly in and/or near the vasculature (Godoy *et al*. 1994; Danyluk *et al*. 1998; Bravo *et al*. 1999; Nylander *et al*. 2001, Hara *et al*. 2011). Studies using

transgenics and mutants have reported the relationship between dehydrin expression and stress tolerance in plants. The overexpression of dehydrin genes in plants enhanced their tolerance to stresses, such as low temperature (Hara *et al*. 2003; Puhakainen *et al*. 2004; Houde *et al*. 2004; Yin *et al*. 2006, Ochoa-Alfaro *et al*. 2012, Xing *et al*. 2011), osmotic stress (Cheng *et al*. 2002; Figueras *et al*. 2004; Brini *et al*. 2007, Wang *et al*. 2011), and high salinity (Shekhawat *et al*., 2011). Reduction of dehydrin contents lowered seed longevity in *Arabidopsis* (Hundertmark *et al*. 2011). Functional studies at the molecular level have attempted to elucidate how dehydrins participate in promoting stress tolerances. Dehydrins showed cryoprotection (see reviews cited above), antifreeze activity (Wisniewski *et al*. 1999), phospholipid binding (Koag *et al*. 2009; Kovacs *et al*. 2008; Eriksson *et al*. 2011), nucleic acid binding (Hara *et al*. 2009; Lin *et al*., 2012), and calcium binding (Heyen *et al*. 2002; Alsheikh *et al*. 2005). However, how these *in vitro* functions are associated with enhancing the stress tolerance in plants remains unknown.

One of the typical phenomena observed in transgenic plants expressing dehydrins is the reduction of lipid peroxidation under stress conditions (Hara *et al*. 2003; Shekhawat *et al*. 2011; Xing *et al*., 2011). It has been shown that the lipid peroxidation results from radical oxygen species (ROS) generated in stressed plants (Shen *et al*., 1997; Iturbe-Ormaetxe *et al*., 1998). Generally, transition metals are thought to be the origins of ROS generation *in vivo* (Iturbe-Ormaetxe *et al*., 1998). Many dehydrins can bind heavy metals with their His-rich sequences (Svensson *et al*. 2000; Krüger *et al*. 2002; Hara *et al*. 2005, Rahman *et al*. 2011). Although it is postulated that dehydrins may control the ROS generation from transition heavy metals like Cu, the ROS-controlling functions of dehydrins have not been demonstrated yet.

In order to investigate whether dehydrins can control the generation of ROS from heavy metals, we focused on KS-type dehydrins. The reasons are as follows: first, the KS-type dehydrins have been well characterized to bind heavy metals. The *Ricinus communis* KS-type dehydrin ITP was identified as a metal transporter that moves through the phloem of young plants (Krüger *et al*. 2002). The *Arabidopsis* KS-type dehydrin AtHIRD11 (At1g54410), which accumulated in the cambial zone of the vasculature, also bound metals (Hara *et al*. 2011). Second, the KS-type dehydrin is the shortest subfamily in length (approximately 100 amino acids); therefore the type has a simple domain constitution, suggesting that, if the KS-type dehydrin can control the ROS generation, the domains that are related to the control can be identified with comparative ease. In this paper, we found that the KS-type dehydrins can reduce the ROS generation from Cu. We also propose that the His contents and the length of the peptides are fundamental factors that influence the strength of ROS reduction by the KS-type dehydrins.

Materials and methods

Preparation of recombinant AtHIRD11

A recombinant AtHIRD11 protein was produced by a method reported previously (Hara *et al*., 2011). In brief, the ORF of AtHIRD11 was inserted into the pET-30 *Escherichia coli* expression system (Novagen, WI, USA). This expression system synthesizes a recombinant protein which has His- and S-tag sequences at the N-terminus. The *E. coli* strain BL21 having the expression construct was precultured at 37°C. The protein

expression, which was induced by the addition of isopropyl β-D-thiogalactopyranoside (1 mM), proceeded for an additional 3 h at 28°C. Bacterial cells (800 ml culture) were lysed by BugBuster reagent (Novagen). The lysate clarified by centrifugation was heated at 90°C for 20 min, and then centrifuged again. The supernatant containing the tagged AtHIRD11 was digested with Factor Xa (Novagen) to remove the tags (His- and S-tags). The tag-less AtHIRD11 protein was purified subsequently by a HiTrap Chelating HP column (1 ml, GE Healthcare, Tokyo, Japan) immobilizing Ni^{2+} and then an anion-exchange column (10 ml, DEAE-Toyopearl 650M, Tosoh, Tokyo, Japan). The sample was desalted using the NAP-25 column (GE Healthcare) and freeze-dried. The dried AtHIRD11 was weighed and stored as a water solution (10 mg ml^{-1}) at -80°C until use. The protein was identified as AtHIRD11 using matrix-assisted laser desorption/ionization-time of flight-mass spectrometry (MALDI-TOF-MS).

Peptide synthesis

In this study, 32 peptides other than AtHIRD11 were chemically synthesized. Their sequences appear in Table 1. Each synthetic peptide has a Trp residue at the N-terminus which allows detection by UV (280 nm) to quantitatively monitor the synthetic peptide. The peptides, which were prepared by an automated solid phase peptide synthesizer (Tetras, Advanced ChemTech, KY, USA), were purified using C18 reversed-phase column chromatography (LC-20AB, Shimadzu, Kyoto, Japan) to 98% homogeneity with a linear gradient of acetonitrile (from 20% to 40%) in 0.1% trifluoro acetic acid solution over 20 min. The purified peptides were identified by MS (LCMS-2020, Shimadzu).

145

146 *Reduction of ROS generation*

147

148 The inhibiting effects of AtHIRD11 and its related domains on ROS generation were
149 measured by the Cu-ascorbate system, which was established for researching the
150 ROS-reducing activities of peptides by detecting hydroxyl radicals (Guilloreau *et al*.
151 2007). This system consisted 1/10 PBS pH 7.4 (13.7 mM NaCl, 0.27 mM KCl, 1 mM
152 Na_2HPO_4, and 0.176 mM KH_2PO_4), desferrioxamine (1 μM), test samples [0-1.85 μM
153 for AtHIRD11, 0-30 μM for peptides containing His, 0-300 μM for peptides without His,
154 0-5 μM for bovine serum albumin (BSA), 0-10 μM for ethylene diamine tetra-acetic acid
155 (EDTA), 0-100 μM for glutathione (GSH), 0-500 μM for His, and 0-2 mM for Gly], $CuCl_2$
156 (4.6 μM), coumarin-3-carboxylic acid (3-CCA, 10 mM), which is a hydroxyl radical
157 detector, and sodium ascorbate (300 μM) in a total volume of 200 μl. The ROS
158 generation was started by the addition of sodium ascorbate, and then the increase in
159 fluorescence (395 nm excitation, 452 nm emission) was monitored for 10 min using a
160 Varioskan Flash microplate reader (Thermo Scientific, Tokyo, Japan) in the kinetic
161 mode. The initial velocity of the increase in fluorescence was measured. In the
162 previous report, the addition of desferrioxamine was recommended because an
163 increase in background fluorescence may occur due to the presence of trace metals in
164 the water used in the experiment (Guilloreau *et al*. 2007). Although our experimental
165 condition did not result in such a background increase, we used desferrioxamine for
166 completeness.

167 Since hydrogen peroxide is also generated in the Cu-ascorbate system (Guilloreau
168 *et al*. 2007), the hydrogen peroxide generation was quantified by the titanium sulfate

method (Eisenberg 1943) with modifications. The test mixture contained 1/10 PBS pH 7.4, desferrioxamine (1 μM), AtHIRD11 (0-1.85 μM), $CuCl_2$ (4.6 μM), and sodium ascorbate (300 μM) in a total volume of 200 μl. After reacting for 3 min, 50 μl of 3% titanium sulfate solution was added to the mixture, and then absorbance at 450 nm was measured using the Varioskan Flash microplate reader. The blank in each case was the mixture containing neither $CuCl_2$ nor sodium ascorbate. Preliminary experiments showed that a reaction period of 3 min was appropriate for measuring the initial velocity of the hydrogen peroxide generation. A calibration curve was produced with the authentic hydrogen peroxide solution.

CD analyses

AtHIRD11 was subjected to a spectropolarimeter (J-820, JASCO) under the presence of metals. AtHIRD11 (4.6 μM) and various concentrations (2.3, 23, and 230 μM) of metals, such as $CaCl_2$, $MgCl_2$, $MnCl_2$, $CoCl_2$, $NiCl_2$, $CuCl_2$, and $ZnCl_2$, were combined in 1/10 PBS pH 7.4. The scan was performed from 195 to 250 nm. The scan speed, resolution, and cell width were 100 nm min^{-1}, 1 nm, and 2 mm, respectively. The obtained data were analyzed by DICHROWEB (http://dichroweb.cryst.bbk.ac.uk/html/home.shtml), which is an online server for predicting secondary structures of proteins (Whitmore and Wallace, 2004).

Protease sensitivity of AtHIRD11

AtHIRD11 (4.6 μM), metals such as $CaCl_2$, $MgCl_2$, $MnCl_2$, $CoCl_2$, $NiCl_2$, $CuCl_2$, and

193 $ZnCl_2$ (2.3, 23, and 230 μM), and trypsin (0.05 μM) were combined in 1/10 PBS pH 7.4.
194 A digestive reaction was started by the addition of trypsin. After the samples were
195 incubated at room temperature for 10 min, the reactions were terminated by heating at
196 95°C. The AtHIRD11 in the samples was resolved by sodium dodecyl
197 sulfate-polyacrylamide gel electrophoresis (SDS-PAGE), and then the gel was stained
198 with colloidal Coomassie blue (Bio-Safe, Bio-Rad, Tokyo, Japan). After the digital
199 images were taken, the intensities of the AtHIRD11 bands were determined by
200 NIH-Image software (http://rsbweb.nih.gov/nih-image/). The intensity of the
201 non-digested AtHIRD11 with no metal was standardized (100%).
202
203 *Self association of AtHIRD11*
204
205 The association degree of AtHIRD11 was determined as follows. AtHIRD11 (4.6 μM)
206 was mixed with metals such as $CaCl_2$, $MgCl_2$, $MnCl_2$, $CoCl_2$, $NiCl_2$, $CuCl_2$, and $ZnCl_2$
207 (2.3, 23, and 230 μM) in 1/10 PBS pH 7.4 (total volume; 40 μl) in siliconized plastic
208 tubes. After being incubated at room temperature for 5 min, the samples were
209 centrifuged at 10000 *g* for 15 min at 4°C. The supernatants were totally transferred to
210 the new tubes, and then the pellets were resuspended in 40 μl of 1/10 PBS by
211 vortexing. AtHIRD11 was resolved by SDS-PAGE. The gel was stained with colloidal
212 Coomassie blue (Bio-Safe). The intensities of the AtHIRD11 bands in the digital
213 images were determined by NIH-Image software. The amount of AtHIRD11 in the
214 pellet was expressed as a percentage. In each sample, the sum of the intensities of
215 AtHIRD11 in the supernatant and the pellet was standardized (100%).
216

Data analysis

Data for *P* values were analyzed by Student's *t* test at a significance level of 0.05. To fit curves through points, the curve-fitting tools in Microsoft Excel 2007 were used.

Results

Reduction of ROS generation from Cu by AtHIRD11

AtHIRD11 (At1g54410) is a KS-type dehydrin consisting of 98 amino acids (Hara *et al*., 2011). AtHIRD11 has a simple domain constitution including K-, PK-, and S-segments (Fig. 1A). Histidine residues frequently occur over the sequence of AtHIRD11. The histidine content of AtHIRD11 (13.3%) is the 7th highest in the open reading frames of the *Arabidopsis* genome (Hara *et al*. 2010). Orthologs of AtHIRD11 are widely spread in higher plants such as *Ricinus communis*, *Glycine max*, *Solanum sogarandinum*, *Oryza sativa*, *Medicago sativa*, *Vitis vinifera,* etc. (Rorat *et al.*, 2004; Hara *et al*., 2011).

In order to test whether AtHIRD11 affects a ROS generation, we prepared the recombinant AtHIRD11 protein that is produced by *Escherichia coli*. We used a common ROS-generating reaction, i.e. the Cu-ascorbate system, which was established to investigate ROS-silencing activity (Guilloreau *et al*. 2007). Ascorbate reduces Cu^{2+} to Cu^{+}, and then Cu^{+} subsequently reduces oxygen to hydroxyl radicals via the formation of superoxide anions and hydrogen peroxide as intermediates under aerobic conditions (Fig. 1B). Through the radical generation, Cu^{+} is regenerated from Cu^{2+} by ascorbate. According to the theory, hydroxyl radicals were generated when

241 ascorbate (300 μM) was combined with Cu^{2+} (4.6 μM) (Fig. 1C, condition 4). However,
242 the addition of AtHIRD11 (0.93 μM) attenuated the radical generation of Cu^{2+} with
243 ascorbate (Fig. 1C, condition 5). In this system, Cu^{2+}, ascorbate, or AtHIRD11 did not
244 generate hydroxyl radicals alone (Fig. 1C, conditions 2, 3, and 6). Neither the
245 combination of AtHIRD11 and Cu nor that of AtHIRD11 and ascorbate generated
246 hydroxyl radicals (Fig. 1C, conditions 7 and 8). These results show that the hydroxyl
247 radical formation, which occurred under the coexistence of ascorbate and Cu^{2+}, was
248 reduced by AtHIRD11.
249 The reduction of the hydroxyl radical generation by AtHIRD11 was dose-dependent,
250 and the ID_{50} value was 0.58 ± 0.18 μM (n=4) (Fig. 2A, left graph). AtHIRD11 also
251 attenuated hydrogen peroxide generation in a dose-dependent manner at the ID_{50} of
252 0.52 ± 0.16 μM (n=4) (Fig. 2A, right graph). The ID_{50} values for the reduction of the
253 hydroxyl radical generation were compared between AtHIRD11 and BSA, EDTA, GSH,
254 His, or Gly (Fig. 2B). EDTA is a strong quencher of ROS generation from the
255 metal-ascorbate system (Saran and Bors 1991). The data indicate that AtHIRD11
256 showed the lowest ID_{50} value among the compounds tested (Fig. 2B).
257
258 *Effect of Cu on the conformation of AtHIRD11*
259
260 Since it has been reported that several dehydrins changed their conformations when
261 binding to metals (Hara *et al*., 2009; Mu *et al*., 2011; Rahman *et al*., 2011), we
262 confirmed whether AtHIRD11 also shows a conformational change induced by Cu^{2+}.
263 The CD analysis showed that AtHIRD11 was likely disordered, because a large
264 negative peak at 200 nm was observed (Fig. 3A, a gray broken line). The addition of

265 Cu^{2+} mitigated the degree of the negative peak at 200 nm in a dose-dependent manner
266 (Fig. 3B). This suggests that in the interaction between AtHIRD11 and Cu^{2+}, more Cu^{2+}
267 results in a greater decrease in disorder. Although such conformational changes of
268 AtHIRD11 also occurred with Co^{2+}, Ni^{2+}, and Zn^{2+}, no change occurred with Ca^{2+}, Mg^{2+},
269 and Mn^{2+} (Fig. 3B). Because AtHIRD11 bound Co^{2+}, Ni^{2+}, Cu^{2+}, and Zn^{2+}, whereas it did
270 not bind Ca^{2+}, Mg^{2+}, and Mn^{2+} (Hara *et al*., 2011), it was indicated that the decrease in
271 disorder was promoted only by the metals which bound to AtHIRD11.
272 The DICHROWEB analysis also indicated that the disordered state of AtHIRD11 was
273 reduced by supplying Cu^{2+} (Fig. 3C, U). On the other hand the analysis showed a
274 decrease in distorted helices (Fig. 3C, H2) and increases in regular and distorted
275 β-strands (Fig. 3C, S1 and S2) as the Cu^{2+} concentration increased, whereas the
276 disordered state was predominant even when the highest concentration of Cu^{2+} was
277 added to AtHIRD11.
278 Metals including Cu^{2+} can induce not only conformational changes but also protease
279 resistance in some disordered proteins such as prion (Lehmann, 2002). Therefore, it is
280 assumed that AtHIRD11 may be converted to protease-resistant forms. Although
281 AtHIRD11 is highly susceptible to trypsin, AtHIRD11 became resistant to protease by
282 the addition of Co^{2+}, Ni^{2+}, Cu^{2+}, and Zn^{2+} (Fig. 4A). On the other hand, Ca^{2+}, Mg^{2+}, and
283 Mn^{2+}, which cannot bind to AtHIRD11, did not enhance the protease resistance. If the
284 molar ratios of Cu^{2+} to AtHIRD11 increased, the degree of trypsin susceptibility
285 decreased (Fig. 4B). Similar results were obtained in the cases of Co^{2+}, Ni^{2+}, and Zn^{2+}.
286 Moreover, the addition of Cu^{2+} increased the association species of AtHIRD11 in a
287 dose-dependent manner (Fig. 5). Co^{2+}, Ni^{2+}, and Zn^{2+} promoted the association of
288 AtHIRD11 like Cu^{2+} did. However, Ca^{2+}, Mg^{2+}, and Mn^{2+} did not.

Domains contributing to the ROS silencing

In order to postulate the mechanisms regarding the reducing activity of the Cu-promoted ROS generation by AtHIRD11, we attempted to determine the functional domains which contribute to the activity. We divided the AtHIRD11 amino acid sequence into 7 domains, i.e., D1 to D7 (Fig. 1A). D1 and D2 are N-terminal sequences which do not contain any conserved segments found in dehydrins. D3, D5, and D7 are conserved K-, polylysine (PK)-, and S-segments, respectively. D4 and D6 are junction regions between the conserved segments (D4; between the K-segment and the PK-segment, D6; between the PK-segment and the S-segment). The seven domains (D1 to D7) and the AtHIRD11 whole sequence were subjected to the Cu-ascorbate system (Table 1, AtHIRD11 and domains). It was indicated that five (D1 to D4, and D6) out of the seven domains showed apparent ROS-reducing activities (less than 10 μM of ID_{50}), suggesting that the functional domains exist through the whole sequence of AtHIRD11. However, we assumed that D6 may be one of the core sequences for expressing the ROS-reducing activity, because this domain showed strong activity despite having the shortest sequence.

Factors determining the ROS-silencing activity

Since the domains containing His apparently showed the ROS-reducing activity as described above, it was suggested that His may be a crucial residue for the activity. To confirm this, we prepared mutant domains in which His residues in the corresponding

original domains were changed to Ala residues (Table 1, Modified domains). The mutant domains were D2H/A, D3H/A, D4H/A, and D6H/A, whose original domains were D2, D3, D4, and D6, respectively. Expectedly, the activities of all four mutant domains were remarkably lower than those of the corresponding original domains. This finding suggests that the presence of His in the domains of AtHIRD11 is important to express efficient ROS-reducing activities.

To search for the factors that determine the magnitude of the ROS-reducing activities, we gathered more data regarding the ROS-reducing activities of the KS-type dehydrin-related peptides which contain various His numbers. In addition to the peptides tested above, we prepared 21 other peptides, i.e., a sequence of D5+D6+D7, seven peptides that were mutant D6 sequences of AtHIRD11, and D6 sequences found in the KS-type dehydrins of 13 plant species (Table 1). The sequences of the D6 domains and their adjacent sites of the K_nS-type dehydrins used in this study are shown in Supplementary Fig. S1. The data regarding the sequences, amino acid numbers, the His numbers, and the ID_{50} values of the 27 peptides that possess at least one His residue are represented in Table 1 with the symbol "✓." Using these data, we searched the combinations of the data items that showed good correlations. Finally, we found that when the indices of the ID_{50} x amino acid number (μM) were plotted against the His contents (%), it is likely that the dots fit the continuous curve for the most part (Fig. 6). We applied several approximation models to fit curves through the dots. Comparison of the R^2 values indicated that a power approximation showed the best fit, i.e., ID_{50} x amino acid number (μM) = 352 x His content (%)$^{-0.74}$ (R^2 = 0.788) (Fig. 6, a broken line). This curve indicated that the value of ID_{50} x amino acid number largely decreased as the His contents increased in the range approximately from 5 to 15%. In

the His contents range extending approximately from 15 to 50%, however, the decreasing slope of the ID_{50} x amino acid number curve was much smaller. When the His contents were higher than 50%, the value of ID_{50} x amino acid number was nearly constant regardless of the His contents. Taken together, Fig. 6 suggests that, if the peptide lengths are assumed to be uniform, the ID_{50} values of the peptides decrease as their His contents increase, whereas the decrease of the ID_{50} values reaches a plateau at more than approximately 50% of the His contents.

Discussion

Although many studies have reported that dehydrin expression provided an enhancement of abiotic stress tolerances in plants (see citations above), the stress-enhancement mechanisms have not been totally elucidated. In plants, one of the common symptoms in abiotic stress responses is physiological damage caused by ROS (Shen *et al*., 1997; Iturbe-Ormaetxe *et al*., 1998). It is believed that reactive transition metals which are released from organelles and enzymes under abiotic stresses are the sources of ROS generation (Iturbe-Ormaetxe *et al*., 1998). Previous results have indicated that dehydrins bound metals (Svensson *et al*. 2000; Krüger *et al*. 2002; Hara *et al*. 2005, Rahman *et al*. 2011), suggesting that dehydrins may stabilize the transition metals by binding them (Hara *et al*., 2005; Sun and Lin, 2010). However, there has been no report which experimentally demonstrated this proposed stabilization. In this paper, we focused on elucidating the ROS-silencing activity of the KS-type dehydrins. We used a common ROS-generating reaction, i.e. the Cu-ascorbate system. The ID_{50} values were 0.58 μM and 0.52 μM for the reductions in

361 the hydroxyl radical generation and hydrogen peroxide generation, respectively. Since
362 the present Cu-ascorbate system was implemented with 4.6 μM Cu^{2+}, these ID_{50}
363 values were obtained when the ratio of [AtHIRD11] : [Cu^{2+}] was approximately 1:8. Our
364 previous data showed that the maximum binding capacity (B_{max}) of AtHIRD11 for Cu^{2+}
365 was 8 (Hara *et al*., 2011). This suggests that AtHIRD11 can efficiently reduce the ROS
366 generation from Cu when the range of the Cu^{2+} concentration is within the binding
367 capacity of AtHIRD11. The typical Cu content in plants is approximately 90 μmol kg^{-1}
368 dry weight, whereas the value is changeable under different growth conditions (Palmer
369 and Guerinot, 2009). On the other hand, the extractable amount of AtHIRD11 protein
370 from the above-ground part of the *Arabidopsis* plant was found to be approximately 10
371 μmol kg^{-1} dry weight (Hara *et al*., 2011). This suggests that AtHIRD11 may effectively
372 reduce the ROS generated from Cu *in planta*, because the ROS-reducing activity is
373 maintained if 1 mol of AtHIRD11 binds 9 mols of Cu^{2+}. It was reported that the *Musa*
374 KS-type dehydrin MpDhn12 complemented the copper-sensitivity of the yeast mutant
375 *delta sod1*, which lacked Cu/Zn superoxide dismutase (Mu *et al*. 2011). This
376 phenomenon might be caused by the ROS silencing activity of MpDhn12 like
377 AtHIRD11.
378 We showed that the conformational changes of AtHIRD11 increased as the
379 concentration of Cu^{2+} was elevated. DICHROWEB analyses suggest that the
380 disordered state decreased while the β-strand content increased when AtHIRD11 was
381 treated with Cu^{2+} (Fig. 3C). The disordered content, however, was still dominant even
382 when Cu^{2+} was supplied at the highest concentration. As the disordered state
383 decreased, AtHIRD11 that was treated with Cu^{2+} showed some association states,
384 because the AtHIRD11 protein was precipitated by centrifugation (Fig. 5) and formed

protease-resistant species (Fig. 4). However, it was unlikely that this association state was a typical aggregation for the following reasons. First, the visible turbidity was not found in the AtHIRD11 solution containing Cu^{2+}. Second, α-helix aggregation, which is monitored on the basis of the decrease of CD at 222 nm (Zhong and Johnson, 1992), was not detected (Supplementary Fig. S2). Third, the result of the 1-anilino-8-naphthalene sulfonate test for indicating the structural transition from disorder to an orderly aggregated state (Tompa, 2009) was negative (Supplementary Fig. S3). Based on these combined findings, we hypothesized that when AtHIRD11 interacts with Cu^{2+}, AtHIRD11 may self-associate by maintaining a respectably disordered state.

The self-association was accelerated when the ratio of [AtHIRD11] : [Cu^{2+}] reached 1 : 50 (Fig. 5). At this concentration ratio, AtHIRD11 no longer reduced the ROS formation. As described above, the reduction of Cu-promoted ROS generation by AtHIRD11 was more effective when the ratio of [AtHIRD11] to [Cu^{2+}] was larger. These results suggest that the magnitude of the ROS-silencing activities of KS-type dehydrins is negatively correlated with the degree of conformational changes in the proteins.

In order to investigate the ROS-reducing domains of AtHIRD11, we determined the reducing activities of the seven domains of AtHIRD11. Five domains (D1, D2, D3, D4, and D6) which contain His showed ROS-reducing activities (Table 1, AtHIRD11 & domains). The mutant domains corresponding to D2, D3, D4, and D6, which contain no His, manifested much lower activities than the original domains (Table 1, Modified domains). This indicates that His is indispensable for the domains to express their efficient ROS-reducing activities. Since dehydrins can bind metals via their His residues (Hara *et al*., 2005; Sun and Lin, 2010), it is likely that the chelating action of

409 Cu^{2+} by His provides the ROS-reducing activities of AtHIRD11. Moreover, we found
410 that the levels of the ROS-reducing activities of the peptides were reflected by the His
411 contents and the amino acid numbers; namely, the indices of ID_{50} x amino acid number
412 (μM) were highly related with the His contents (%) (Fig. 6). A comparison of the
413 ROS-reducing activities of the peptides on the basis of constant amino acid numbers
414 showed that the ID_{50} values decreased as the His contents increased. Intriguingly,
415 however, the decrease in the ID_{50} values weakened when the His contents surpassed
416 20%, and then the decrease reached a plateau at a low level when the His contents
417 surpassed 50%. This indicates that the effects of the His contents on the enhancement
418 of ROS-reducing activity leveled off at more than 20% of the contents. Since His is one
419 of the most expensive amino acids to biosynthesize (Rees et al., 2009), the production
420 of peptides possessing extremely high His contents is likely to be costly for plants.
421 Considering the metabolic cost of His biosynthesis, a level of His contents of
422 approximately 20% is likely to be sufficient for efficient ROS reduction. Indeed, the
423 open reading frame which shows the highest His contents in the *Arabidopsis* genome
424 was At5g53590, whose His content was 19.7% (Hara *et al*., 2010).
425 The sixth domain, D6, which showed high ROS-silencing activity, was located
426 between the PK- and S-segments of AtHIRD11 (Fig. 1A). The D6-like sequences were
427 found in all KS-type dehydrins that we checked in the open databases. Various D6
428 sequences which are shown in Supplementary Fig. S1 are suggested to contain mainly
429 His, and subsequently Asp and Gly. Such His-rich sequences are found in the metal
430 transporters of many organisms. For instance, *Arabidopsis* AtMTP1 belonging to the
431 cation diffusion facilitator family has a His-rich loop which may function as a buffering
432 pocket for Zn^{2+} (Kawachi *et al*., 2008). Our results suggest that the His-rich loop may

serve a role in protecting the transportation machinery from damage by ROS by binding transition metals.

The KS-type dehydrin is the smallest subfamily that consists of simple domain constitutions. This suggests that the KS-type dehydrin may be a prototype of other dehydrin subfamilies. Accordingly, the present results regarding the ROS reduction by KS-type dehydrins may be useful for finding dehydrins that show higher ROS-silencing activities. *Arabidopsis* possesses 10 copies of dehydrin genes (Hundertmark and Hincha 2008). Among them, the His-rich dehydrin Lti30 (At3g50970), which is responsive to cold stress, shows the highest His content (13.5%). Although the His content of Lti30 is similar to that of AtHIRD11 (13.3%), the size of Lti30 (193 amino acids) was approximately double that of AtHIRD11 (98 amino acids). This suggests that Lti30 may show more potent ROS-silencing activity (i.e., the lower ID_{50} value) than AtHIRD11, if the correlation between the indices of ID_{50} x amino acid number (μM) and the His contents (%) described in Fig. 6 is taken into consideration. Since it was recently reported that Lti30 could bind to membranes (Eriksson *et al*., 2011), Lti30 may protect membranes from the metals-promoting lipid peroxidation by binding the metals on the surfaces of the membranes. Alternatively, in the presence of metals, Lti30 may be released from the membranes by sequestering the metals from the membranes, because His residues that are associated with the membrane binding may be shielded by the metals.

In conclusion, we propose that His-rich peptides which inhibit the generation of ROS from metals exist in the plant kingdom. Some kinds of dehydrins including the KS-types may be such His-rich ROS-silencing peptides. Moreover, we found a common method of predicting the levels of the ROS-reducing activities of such peptides by using indices

of the His contents and the amino acid numbers. These findings may be useful in elucidating the functions of the His-rich proteins and domains.

Supplementary materials

Supplementary data are available at *JXB* online.

Supplementary Fig. S1. Amino acid sequences of D5s, D6s, and D7s in different K_nS-type dehydrins.

Supplementary Fig. S2. Effect of Cu^{2+} on CD at 222 nm of AtHIRD11.

Supplementary Fig. S3. Effect of Cu^{2+} on the formation of ordered aggregation in AtHIRD11.

Acknowledgements

We thank Prof. Naoto Oku (University of Shizuoka) for helpful discussions. This study was supported in part by a Grant-in-Aid (No. 23380192) for Scientific Research from the Ministry of Education, Science, Sports and Culture of Japan.

References

Alsheikh MK, Svensson JT, Randall SK. 2005. Phosphorylation regulated ion-binding is a property shared by the acidic subclass dehydrins. *Plant, Cell & Environment* **28**, 1114-1122.

Battaglia M, Olvera-Carrillo Y, Garciarrubio A, Campos F, Covarrubias AA. 2008. The enigmatic LEA proteins and other hydrophilins. *Plant Physiology* **148**, 6-24.

Bravo LA, Close TJ, Corcuera LJ, Guy CL. 1999. Characterization of an 80-kDa dehydrin-like protein in barley responsive to cold acclimation. *Physiologia Plantarum* **106**, 177-183.

Brini F, Hanin M, Lumbreras V, Amara I, Khoudi H, Hassairi A, Pagès M, Masmoudi K. 2007. Overexpression of wheat dehydrin DHN-5 enhances tolerance to salt and osmotic stress in *Arabidopsis thaliana*. *Plant Cell Reports* **26**, 2017-2026.

Cheng Z, Targolli J, Huang X, Wu R. 2002. Wheat LEA genes, PMA80 and PMA1959 enhance dehydration tolerance of transgenic rice (*Oryza sativa* L.). *Molecular Breeding* **10**, 71-82.

Close TJ. 1996. Dehydrins: Emergence of a biochemical role of a family of plant dehydration proteins. *Physiologia Plantarum* **97**, 795-803.

Danyluk J, Perron A, Houde M, Limin A, Fowler B, Benhamou N, Sarhan F. 1998. Accumulation of an acidic dehydrin in the vicinity of the plasma membrane during cold acclimation of wheat. *The Plant Cell* **10**, 623-638.

Eisenberg G. 1943. Colorimetric Determination of Hydrogen Peroxide. *Industrial and Engineering Chemistry, Analytical Edition* **15**, 327-328.

Eriksson SK, Harryson P. 2011. Dehydrins: Molecular Biology, Structure and Function.

In: U Lüttge, E Beck, D Bartels, eds. *Plant Desiccation Tolerance*. Berlin Heidelberg: Springer, 289-305.

Eriksson SK, Kutzer M, Procek J, Gröbner G, Harryson P. 2011. Tunable membrane binding of the intrinsically disordered dehydrin Lti30, a cold-induced plant stress protein. *The Plant Cell* **23**, 2391-2404.

Figueras M, Pujal J, Saleh A, Save R, Pagès M, Goday A. 2004. Maize Rabl7 overexpression in *Arabidopsis* plants promotes osmotic stress tolerance. *Annals of Applied Biology* **144**, 251-257.

Godoy JA, Lunar R, Torres-Schumann S, Moreno J, Rodrigo RM, Pintor-Toro JA. 1994. Expression, tissue distribution and subcellular localization of dehydrin TAS14 in salt-stressed tomato plants. *Plant Molecular Biology* **26**, 1921-1934.

Guilloreau L, Combalbert S, Sournia-Saquet A, Mazarguil H, Faller P. 2007. Redox chemistry of copper-amyloid-beta: the generation of hydroxyl radical in the presence of ascorbate is linked to redox-potentials and aggregation state. *Chembiochem* **23**, 1317-1325.

Hara M. 2010. The multifunctionality of dehydrins: An overview. *Plant Signaling & Behavior* **5**, 503-508.

Hara M, Fujinaga M, Kuboi T. 2005. Metal binding by citrus dehydrin with histidine-rich domains. *Journal of Experimental Botany* **56**, 2695-2703.

Hara M, Kashima D, Horiike T, Kuboi T. 2010. Metal-binding characteristics of the protein which shows the highest histidine content in the *Arabidopsis* genome. *Plant Biotechnology* **27**, 475-480.

Hara M, Shinoda Y, Kubo M, Kashima D, Takahashi I, Kato T, Horiike T, Kuboi T. 2011. Biochemical characterization of the *Arabidopsis* KS-type dehydrin protein, whose

gene expression is constitutively abundant rather than stress dependent. *Acta Physiologiae Plantarum* **33**, 2103-2116.

Hara M, Shinoda Y, Tanaka Y, Kuboi T. 2009. DNA binding of citrus dehydrin promoted by zinc ion. *Plant, Cell & Environment* **32**, 532-541.

Hara M, Terashima S, Fukaya T, Kuboi T. 2003. Enhancement of cold tolerance and inhibition of lipid peroxidation by citrus dehydrin in transgenic tobacco. *Planta* **217**, 290-298.

Heyen BJ, Alsheikh MK, Smith EA, Torvik CF, Seals DF, Randall SK. 2002. The calcium-binding activity of a vacuole-associated, dehydrin-like protein is regulated by phosphorylation. *Plant Physiology* **130**, 675-687.

Houde M, Dallaire S, N'Dong D, Sarhan F. 2004. Overexpression of the acidic dehydrin WCOR410 improves freezing tolerance in transgenic strawberry leaves. *Plant Biotechnology Journal* **2**, 381-387.

Hundertmark M, Buitink J, Leprince O, Hincha DK. 2011. The reduction of seed-specific dehydrins reduces seed longevity in *Arabidopsis thaliana*. *Seed Science Research* **21**, 165-173.

Hundertmark M, Hincha DK. 2008. LEA (Late Embryogenesis Abundant) proteins and their encoding genes in *Arabidopsis thaliana*. *BMC Genomics* **9**, 118.

Iturbe-Ormaetxe I, Escuredo PR, Arrese-Igor C, Becana M. 1998. Oxidative damage in pea plants exposed to water deficit or paraquat. *Plant Physiology* **116**, 173–181.

Kawachi M, Kobae Y, Mimura T, Maeshima M. 2008. Deletion of a histidine-rich loop of AtMTP1, a vacuolar Zn^{2+}/H^{+} antiporter of *Arabidopsis thaliana*, stimulates the transport activity. *The Journal of Biological Chemistry* **283**, 8374-8383.

Koag MC, Wilkens S, Fenton RD, Resnik J, Vo E, Close TJ. 2009. The K-segment of

maize DHN1 mediates binding to anionic phospholipid vesicles and concomitant structural changes. *Plant Physiology* **150**, 1503-1514.

Kovacs D, Kalmar E, Torok Z, Tompa P. 2008. Chaperone activity of ERD10 and ERD14, two disordered stress-related plant proteins. *Plant Physiology* **147**, 381-390.

Krüger C, Berkowitz O, Stephan UW, Hell R. 2002. A metal-binding member of the late embryogenesis abundant protein family transports iron in the phloem of *Ricinus communis* L. *The Journal of Biological Chemistry* **277**, 25062-25069.

Lehmann S. 2002. Metal ions and prion diseases. *Current Opinion in Chemical Biology* **6**, 187-192.

Lin CH, Peng PH, Ko CY, Markhart AH, Lin TY. 2012. Characterization of a novel Y_2K-type dehydrin VrDhn1 from *Vigna radiate*. *Plant & Cell Physiology* First published online.

Mu P, Feng D, Su J, Zhang Y, Dai J, Jin H, Liu B, He Y, Qi K, Wang H, Wang J. 2011. Cu^{2+} triggers reversible aggregation of a disordered His-rich dehydrin MpDhn12 from *Musa paradisiaca*. *The Journal of Biochemistry* **150**, 491-499.

Nylander M, Svensson J, Palva ET, Welin BV. 2001. Stress-induced accumulation and tissue-specific localization of dehydrins in *Arabidopsis thaliana*. *Plant Molecular Biology* **45**, 263-279.

Ochoa-Alfaro AE, Rodríguez-Kessler M, Pérez-Morales MB, Delgado-Sánchez P, Cuevas-Velazquez CL, Gómez-Anduro G, Jiménez-Bremont JF. 2012. Functional characterization of an acidic SK_3 dehydrin isolated from an *Opuntiastreptacantha* cDNA library. *Planta* **235**, 565-578.

Palmer CM, Guerinot ML. 2009. Facing the challenges of Cu, Fe and Zn homeostasis in plants. *Nature Chemical Biology* **5**, 333-340.

Puhakainen T, Hess MW, Mäkelä P, Svensson J, Heino P, Palva ET. 2004. Overexpression of multiple dehydrin genes enhances tolerance to freezing stress in Arabidopsis. *Plant Molecular Biology* **54**, 743-753.

Rahman LN, Smith GS, Bamm VV, Voyer-Grant JA, Moffatt BA, Dutcher JR, Harauz G. 2011. Phosphorylation of *Thellungiella salsuginea* dehydrins TsDHN-1 and TsDHN-2 facilitates cation-induced conformational changes and actin assembly. *Biochemistry* **50**, 9587-9604.

Rees JD, Ingle RA, Smith JA. 2009. Relative contributions of nine genes in the pathway of histidine biosynthesis to the control of free histidine concentrations in *Arabidopsis thaliana*. *Plant Biotechnology Journal* **7**, 499-511.

Rorat T. 2006. Plant dehydrins: tissue location, structure and function. *Cellular and Molecular Biology Letters* **11**, 536-556.

Rorat T, Grygorowicz WJ, Irzykowski W, Rey P. 2004. Expression of KS-type dehydrins is primarily regulated by factors related to organ type and leaf developmental stage during vegetative growth. *Planta* **218**, 878-885.

Saran M, Bors W. 1991. Direct and indirect measurements of oxygen radicals. *Klinische Wochenschrift* **69**, 957-964.

Shekhawat UK, Srinivas L, Ganapathi TR. 2011. MusaDHN-1, a novel multiple stress-inducible SK(3)-type dehydrin gene, contributes affirmatively to drought- and salt-stress tolerance in banana. *Planta* **234**, 915-932.

Shen B, Jensen RG, Bohnert HJ. 1997. Mannitol protects against oxidation by hydroxyl radicals. *Plant Physiology* **115**, 527–532.

Sun X, Lin HH. 2010. Role of plant dehydrins in antioxidation mechanisms. *Biologia* **65**, 755-759.

Svensson J, Ismail AM, Palva ET, Close TJ. 2002. Dehydrins. In: KB Storey, JM Storey, eds. *Sensing, Signaling and Cell Adaptation*. Amsterdam: Elsevier, 155-171.

Svensson J, Palva ET, Welin B. 2000. Purification of recombinant *Arabidopsis thaliana* dehydrins by metal ion affinity chromatography. *Protein Expression and Purification* **20**, 169-178.

Tompa P. 2009. *Structure and function of intrinsically disordered proteins*. Florida: CRC Press.

Tunnacliffe A, Wise MJ. 2007. The continuing conundrum of the LEA proteins. *Naturwissenschaften* **94**, 791-812.

Wang Y, Wang H, Li R, Ma Y, Wei J. 2011. Expression of a SK2-type dehydrin gene from *Populus euphratica* in a *Populus tremula* × *Populus alba* hybrid increased drought tolerance. *African Journal of Biotechnology* **10**, 9225-9232.

Whitmore L, Wallace BA. 2004. DICHROWEB, an online server for protein secondary structure analyses from circular dichroism spectroscopic data. *Nucleic Acids Research* **32** (Web Server issue), W668-673.

Wisniewski M, Webb R, Balsamo R, Close TJ, Yu XM, Griffith M. 1999. Purification, immunolocalization, cryoprotective, and antifreeze activity of PCA60: A dehydrin from peach (*Prunus persica*). *Physiologiae Plantarum* **105**, 600-608.

Xing X, Liu Y, Kong X, Liu Y, Li D. 2011. Overexpression of a maize dehydrin gene, *ZmDHN2b*, in tobacco enhances tolerance to low temperature. *Plant Growth Regulation* **65**, 109-118.

Yin Z, Rorat T, Szabala BM, Ziólkowska A, Malepszy S. 2006. Expression of a *Solanum sogarandinum* SK_3-type dehydrin enhances cold tolerance in transgenic cucumber seedlings. *Plant Science* **170**, 1164-1172.

Zhong L, Johnson WC Jr. 1992. Environment affects amino acid preference for secondary structure. *Proceedings of the National Academy of Sciences of the United States of America* **89**, 4462-4465.

Table 1. His contents and radical-reducing activities of KS-type dehydrin-related peptides

Fifty percent inhibitory dose (ID_{50}) values were determined by the ROS generation reaction using the Cu-ascorbate system. Ascorbate (300 μM) and $CuCl_2$ (4.6 μM) were used. Four replicates.

Peptide names	Sequences	Species	AANs*	His numbers	His contents (%)	ID_{50} (μM)		ID_{50} x AAN* (μM)		Used in Fig. 6
						Average	SD	Average	SD	
AtHIRD11 & domains										
AtHIRD11	D1+D2+D3+D4+D5+D6+D7	*Arabidopsis thaliana*	98	13	13.3	0.58	0.18	56.85	17.66	✓
D1	WMAGLINKIGDALHIGGGNKEG	*Arabidopsis thaliana*	22	1	4.5	9.59	0.67	211.0	14.7	✓
D2	WEHKKEEEHKKHVDEHKSGE	*Arabidopsis thaliana*	20	4	20.0	1.50	0.02	30.03	0.50	✓
D3	WHKEGIVDKIKDKIHG	*Arabidopsis thaliana*	16	2	12.5	3.32	0.11	53.08	1.78	✓
D4	WGEGKSHDGEGKSHDG	*Arabidopsis thaliana*	16	2	12.5	3.78	0.14	60.52	2.24	✓
D5	WEKKKKKDKKEKK	*Arabidopsis thaliana*	13	0	0.0	195	3	2535	39	
D6	WHHDDGHH	*Arabidopsis thaliana*	8	4	50.0	1.88	0.05	15.07	0.42	✓
D7	WSSSSDSDSD	*Arabidopsis thaliana*	10	0	0.0	75.1	4.2	751.0	42.0	
D5+D6+D7	WEKKKKKDKKEKKHHDDGHHSSSSDSDSD	*Arabidopsis thaliana*	29	4	13.8	1.47	0.05	42.74	1.54	✓
Modified domains										
D2H/A	WEAKKEEEAKKAVDEAKSGE		20	0	0.0	147	14	2940	270	
D3H/A	WAKEGIVDKIKDKIAG		16	0	0.0	223	64	3568	1016	
D4H/A	WGEGKSADGEGKSADG		16	0	0.0	144	32	2304	509	
D6H/A	WAADDGAA		8	0	0.0	196	4	1568	28	
D6 modified										
D6 D/A	WHHAAGHH		8	4	50.0	3.20	0.03	25.59	0.28	✓
D6 D/N	WHHNNGHH		8	4	50.0	1.85	0.10	14.78	0.82	✓
D6 D/H1	WHHHDGHH		8	5	62.5	3.13	0.10	25.01	0.80	✓
D6 D/H2	WHHHHGHH		8	6	75.0	2.32	0.19	18.55	1.49	✓
D6 D/H3	WHHHHHHH		8	7	87.5	3.14	0.41	25.14	3.26	✓
D6×2	WHHDDGHHDDGHH		13	6	46.2	1.35	0.13	17.52	1.63	✓
D6×3	WHHDDGHHDDGHHDDGHH		18	8	44.4	0.95	0.04	17.04	0.67	✓
D6 other plants										
OsD6	WHGEEGHHHDGH	*Oryza sativa*	12	5	41.7	1.69	0.20	20.25	2.37	✓
RrD6	WHEHGHEHGHD	*Retama raetam*	11	5	45.5	1.75	0.20	19.28	2.15	✓
GmD6	WHGHDHHGH	*Glycine max*	9	5	55.6	2.11	0.17	19.01	1.50	✓
SbD6	WHGEGHDHDGH	*Sorghum bicolor*	11	4	36.4	1.85	0.25	20.35	2.78	✓
MsD6	WHGEGHEHGH	*Medicago sativa*	10	4	40.0	2.18	0.19	21.82	1.92	✓
CpD6	WHDEHGHDGH	*Carica papaya*	10	4	40.0	2.52	0.06	25.22	0.64	✓
BdD6	WHGEGHKKEDGH	*Brachypodium distachyon*	12	3	25.0	2.75	0.33	33.03	3.95	✓
VvD6	WHEDGHDHGG	*Vaccinium vitis*	10	3	30.0	3.01	0.50	30.09	5.01	✓
CmD6	WHGEGHKHG	*Corylus mandshurica*	9	3	33.3	2.40	0.12	21.64	1.09	✓
RcD6	WHEHGH	*Ricinus communis*	6	3	50.0	2.87	0.11	17.19	0.68	✓
HvD6	WDGEGHKDDDGH	*Hordeum vulgare*	12	2	16.7	2.66	0.07	31.86	0.80	✓
PmD6	WHGEGHDGG	*Plantago major*	9	2	22.2	3.18	0.18	28.62	1.65	✓
CuD6	WHEDGHE	*Citrus unshiu*	7	2	28.6	4.19	0.44	29.32	3.07	✓

*AAN means amino acid number

Figure Legends

Fig. 1. Reduction of ROS generation from Cu by AtHIRD11. (A) Domain constitution of AtHIRD11. The amino acid sequence was divided into seven domains (D1 - D7). D3, D5, and D7 are K-, PK-, and S-segments, respectively, which are found in many dehydrins. (B) A scheme of the Cu-ascorbate system used in this study. (C) Hydroxyl radical generation under different conditions of the ROS generation system. Eight combinations were tested. AtHIRD11 (0.93 μM), ascorbate (300 μM), and $CuCl_2$ (4.6 μM) were used. Values and bars indicate means and SD of four measurements, respectively.

Fig. 2. Reducing activities of ROS generation by AtHIRD11 and other compounds. (A) Dose-dependent reductions of the ROS generation by AtHIRD11. Results regarding hydroxyl radicals (left graph) and hydrogen peroxide (right graph) are shown. Ascorbate (300 μM) and $CuCl_2$ (4.6 μM) were used. (B) Reducing activities of the generation of hydroxyl radicals by different compounds. AH11, BSA, EDTA, GSH, His, and Gly represent AtHIRD11, bovine serum albumin, ethylene diamine tetra-acetic acid, glutathione, histidine, and glycine, respectively. Values and bars indicate means and SD of four measurements, respectively. Significant difference ($p < 0.05$) in comparison to the value of AtHIRD11 was determined by Student's t-test (* in B).

Fig. 3. Conformational alterations of AtHIRD11 by metals. (A) Circular dichroism (CD) analyses using AtHIRD11 with different concentrations of Cu^{2+}. AtHIRD11 alone (4.6 μM) is shown by a gray broken line. The [AtHIRD11] : [Cu^{2+}] ratios are 1 : 0.5 (4.6 μM :

2.3 μM, a gray solid line), 1 : 5 (4.6 μM : 23 μM, a black broken line), and 1 : 50 (4.6 μM : 230 μM, a black solid line). Values are means of four measurements. (B) Effects of different metal cations on conformational changes of AtHIRD11. CD values at 200 nm are compared. The white column showing the value without metal (NM) is standardized (100%). The [AtHIRD11] : [Cu^{2+}] ratios are 1 : 0.5 (light gray columns), 1 : 5 (dark gray columns), and 1 : 50 (black columns). The concentrations of AtHIRD11 and Cu^{2+} were the same as above. (C) Composition of secondary structures in AtHIRD11 as predicted by DICHROWEB (http://dichroweb.cryst.bbk.ac.uk/html/home.shtml). H1, H2, S1, S2, T, and U indicate regular helix, distorted helix, regular β-strand, distorted β-strand, turn, and unordered contents, respectively. The white columns represent the value without metal. The [AtHIRD11] : [Cu^{2+}] ratios are 1 : 0.5 (light gray columns), 1 : 5 (dark gray columns), and 1 : 50 (black columns). The concentrations of AtHIRD11 and Cu^{2+} were the same as above. In (B) and (C), values and bars indicate means and SD of four measurements, respectively. *Significant difference ($p < 0.05$) in comparison to the value without metal was determined by Student's t-test.

Fig. 4. Effects of metals on trypsin resistance of AtHIRD11. AtHIRD11 (4.6 μM) was treated with trypsin (0.05 μM) after metal ions were added. (A) AtHIRD11 treated with trypsin was resolved by SDS-PAGE. The gel was stained with colloidal Coomassie blue. Open triangles represent levels of metal concentrations. In each metal, the concentration increases from left to right in three steps. The [AtHIRD11] : [Cu^{2+}] ratios are 1 : 0.5 (4.6 μM : 2.3 μM, left), 1 : 5 (4.6 μM : 23 μM, middle), and 1 : 50 (4.6 μM : 230 μM, right). NMC indicates AtHIRD11 alone which was treated with neither metal nor trypsin. NM means AtHIRD11 treated with trypsin but without metal. Arrowheads show

the size of AtHIRD11. (B) Relative intensities of the AtHIRD11 bands. The band intensity of the NMC condition is standardized (100%). The [AtHIRD11] : [metals] ratios are 1 : 0.5 (light gray columns), 1 : 5 (dark gray columns), and 1 : 50 (black columns). The concentrations of AtHIRD11 and Cu^{2+} were the same as above. Values and bars indicate means and SD of four measurements, respectively. *Significant difference (p < 0.05) in comparison to the NM condition (white bar) was determined by Student's t-test.

Fig. 5. Effects of metals on association species formation of AtHIRD11. Different kinds of metals were added to the AtHIRD11 solutions (4.6 μM), and then the mixtures were centrifuged. The resultant supernatants (Sup) and pellets (Ppt) were resolved by SDS-PAGE. (A) The SDS-PAGE gel was stained with colloidal Coomassie blue. Open triangles represent levels of metal concentrations. In each metal, the concentration increases from left to right in three steps. The [AtHIRD11] : [Cu^{2+}] ratios are 1 : 0.5 (4.6 μM : 2.3 μM, left), 1 : 5 (4.6 μM : 23 μM, middle), and 1 : 50 (4.6 μM : 230 μM, right). NM indicates AtHIRD11 alone (without metal). Arrowheads show the size of AtHIRD11. (B) Relative intensities of the AtHIRD11 bands in the pellet fractions. The sums of band intensities in supernatants and those in pellets are expressed as 100%. The [AtHIRD11] : [metals] ratios are 1:0.5 (light gray columns), 1:5 (dark gray columns), and 1:50 (black columns). The concentrations of AtHIRD11 and Cu^{2+} were the same as above. Values and bars indicate means and SD of four measurements, respectively. *Significant difference (p < 0.05) in comparison to the NM condition (a white bar) was determined by Student's t-test.

Fig. 6. Relationships between His contents (%) and ID_{50} x amino acid number values

(μM) in the 27 KS-dehydrin-related peptides. The His contents (x-axis) were plotted against the ID_{50} x amino acid number values (y-axis). Values in Table 1 are used to make this graph. Values and bars indicate means and SD of four measurements, respectively. The regression line ($y = 352x^{-0.74}$, $R^2 = 0.788$) was shown with a broken line.

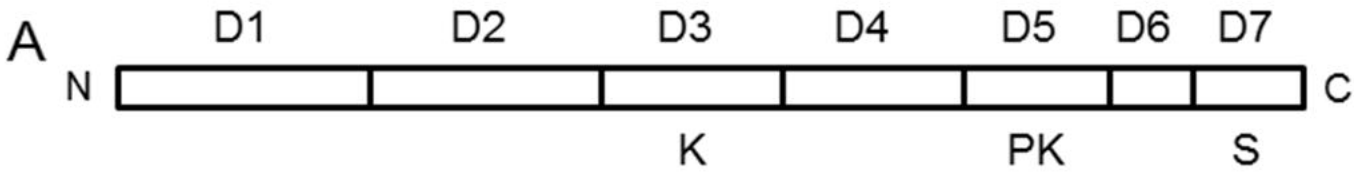

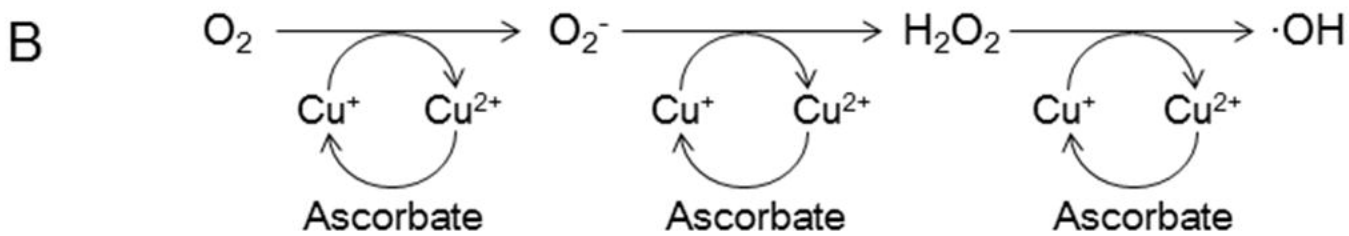

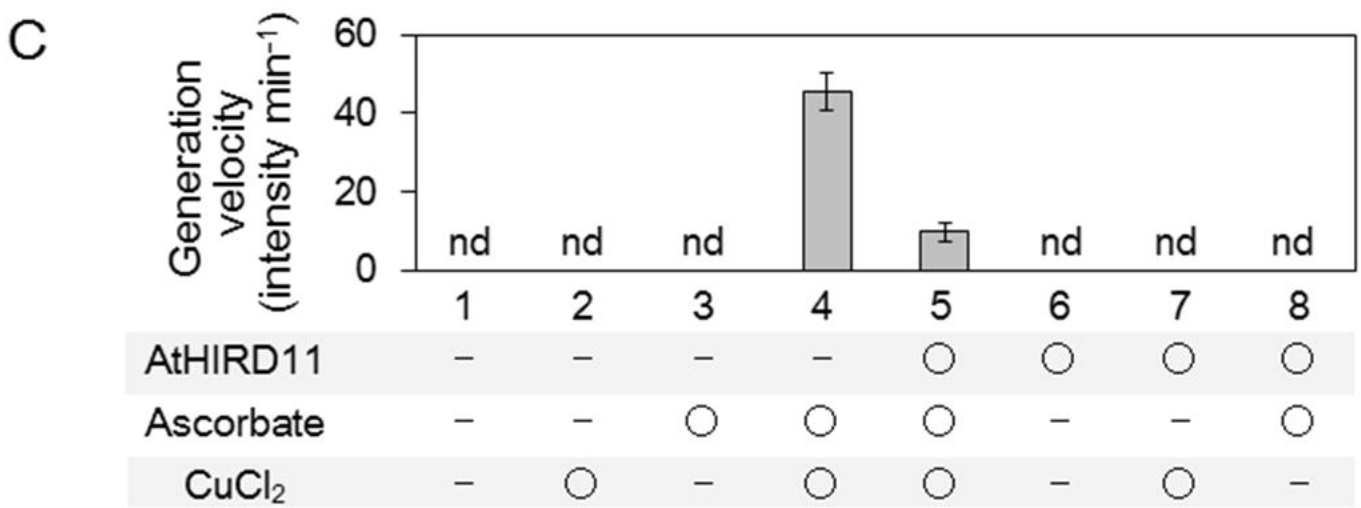

Fig. 1 Hara et al.

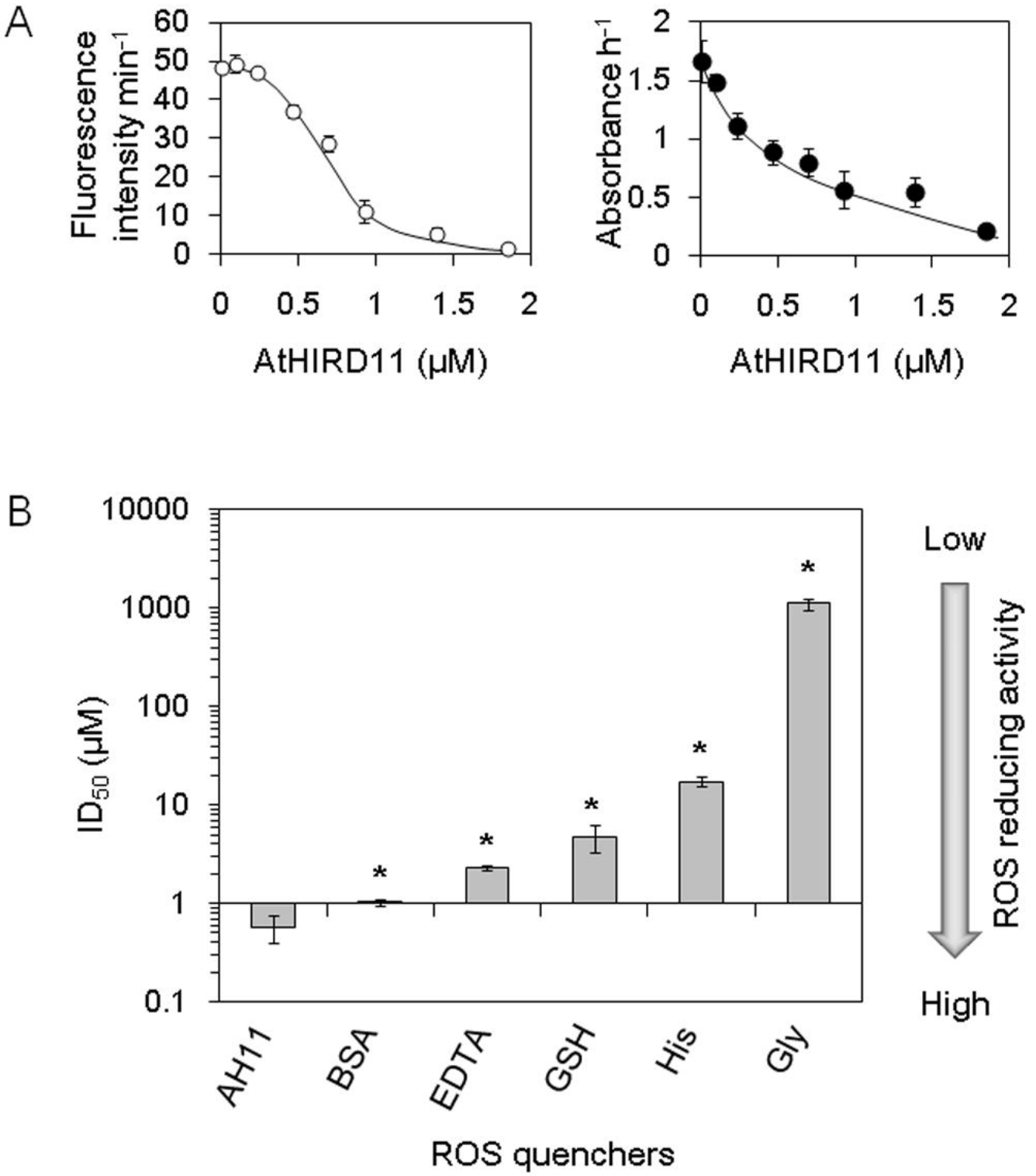

Fig. 2 Hara et al.

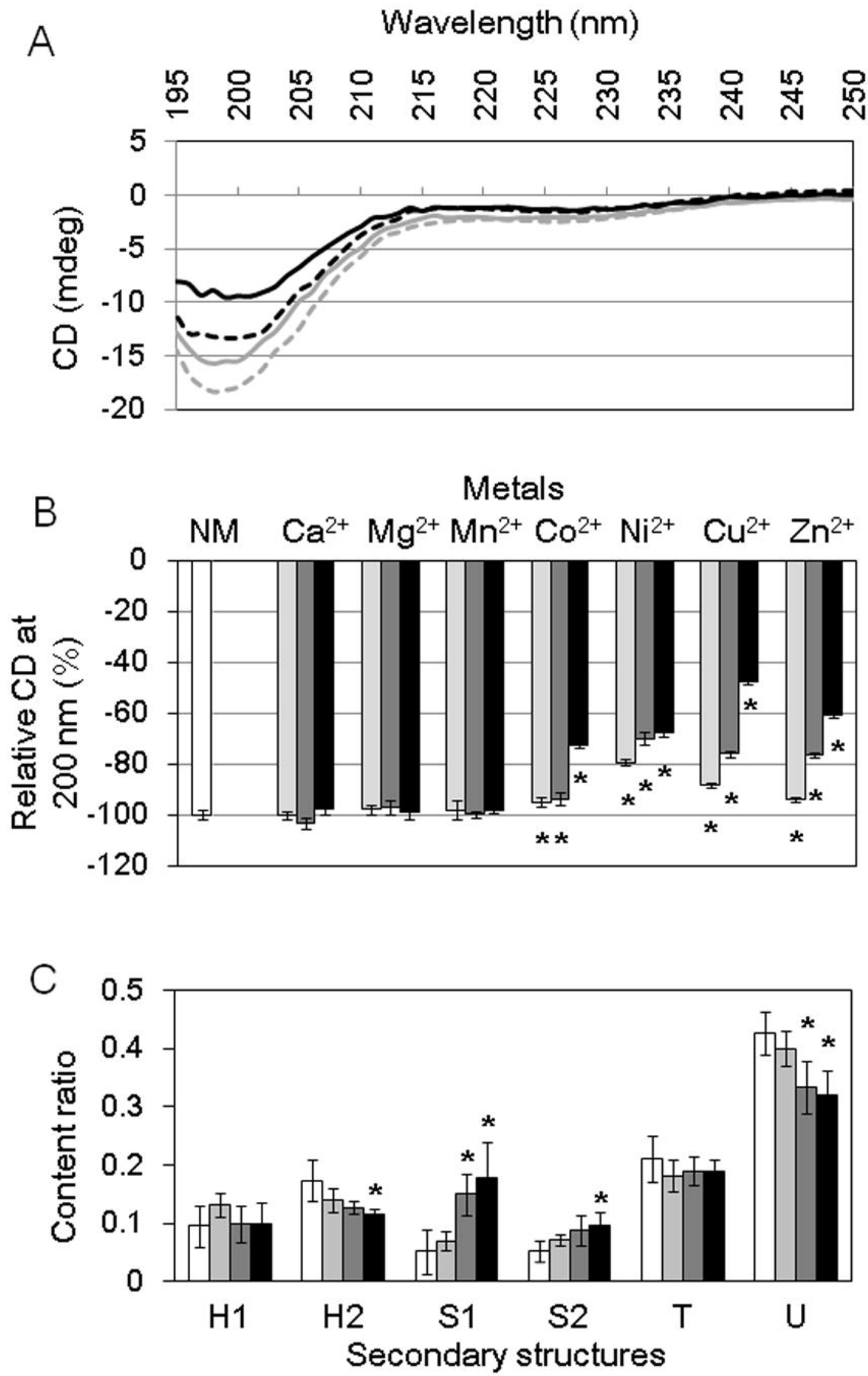

Fig. 3 Hara et al.

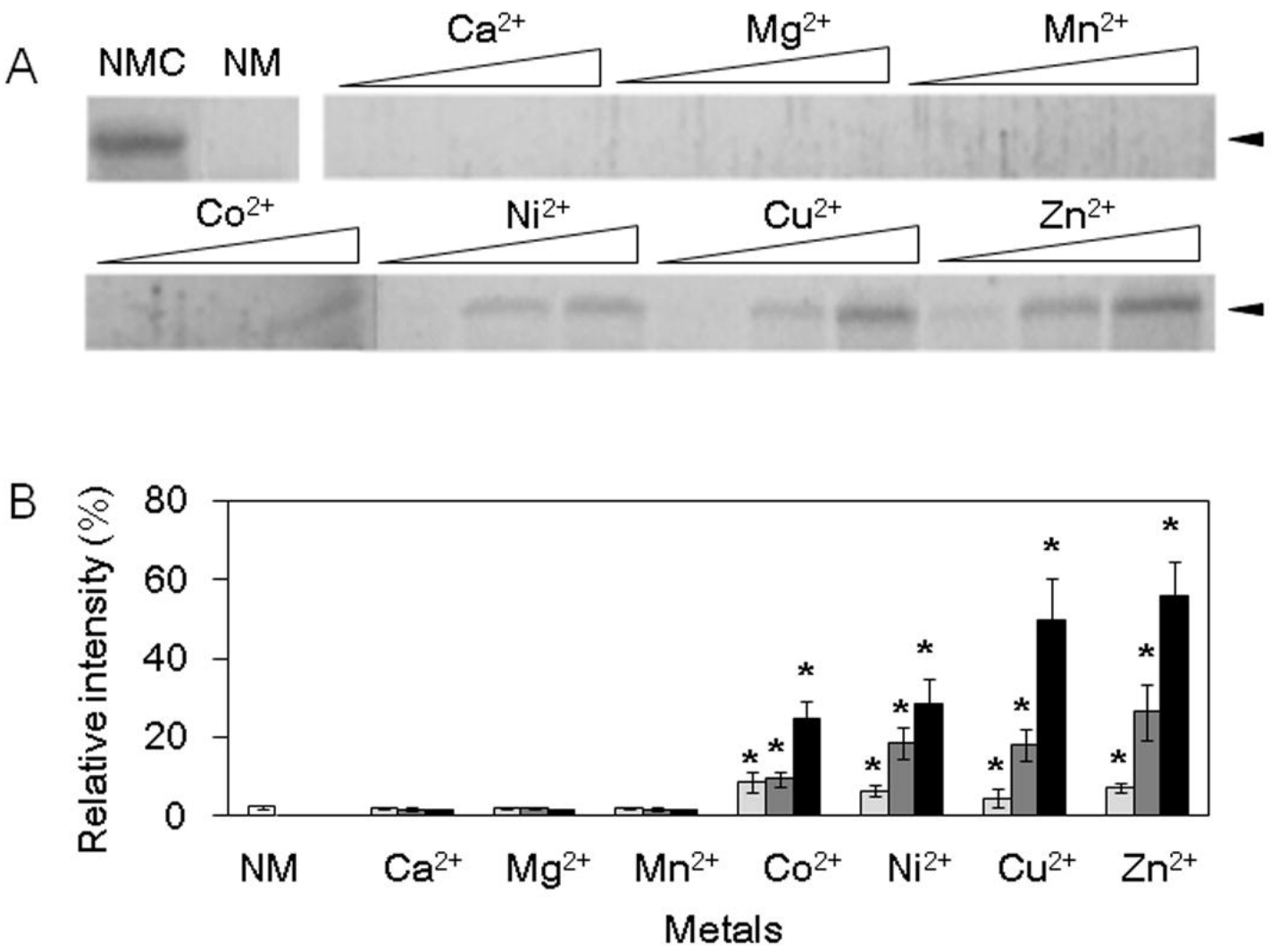

Fig. 4 Hara et al.

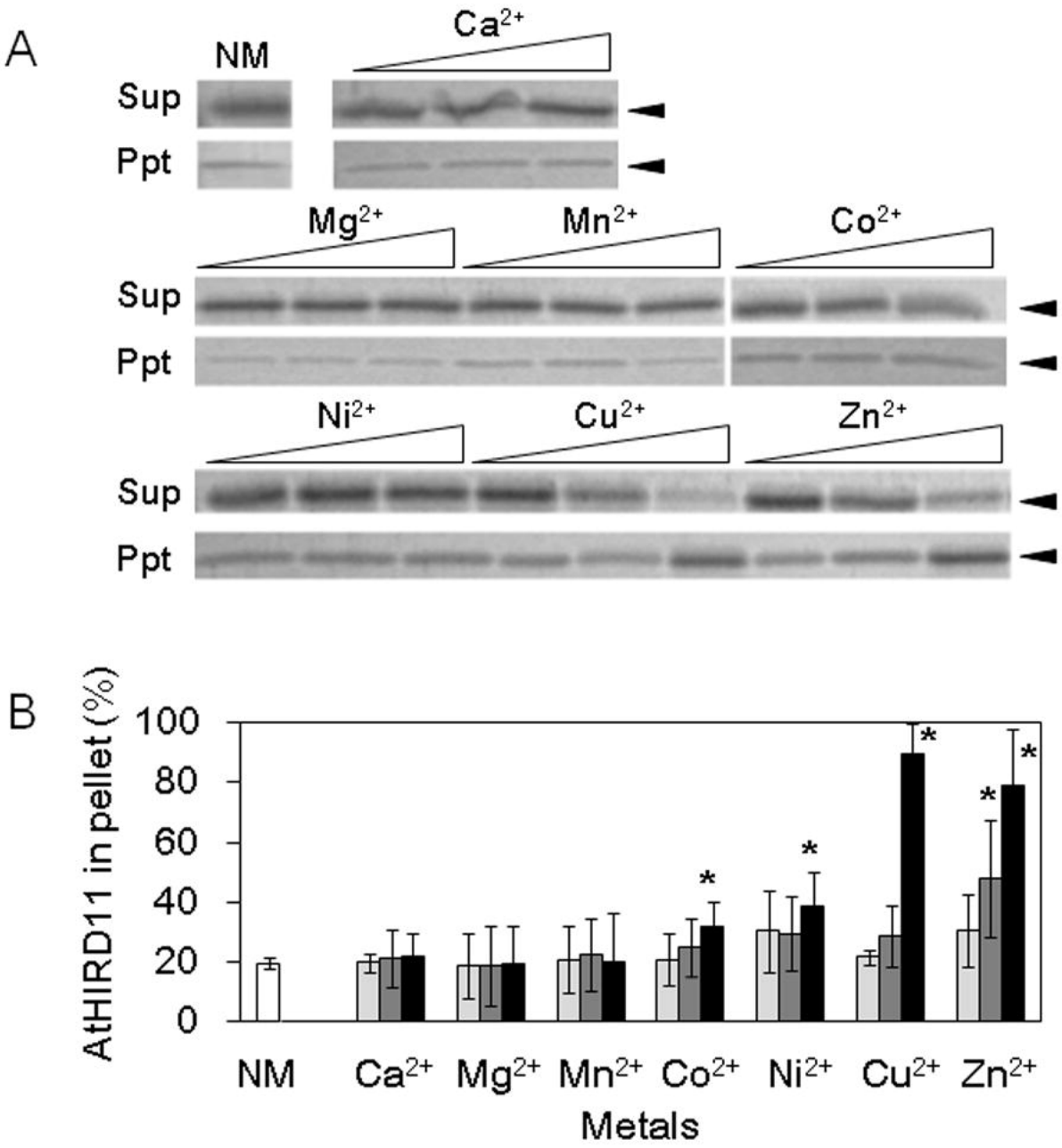

Fig. 5 Hara et al.

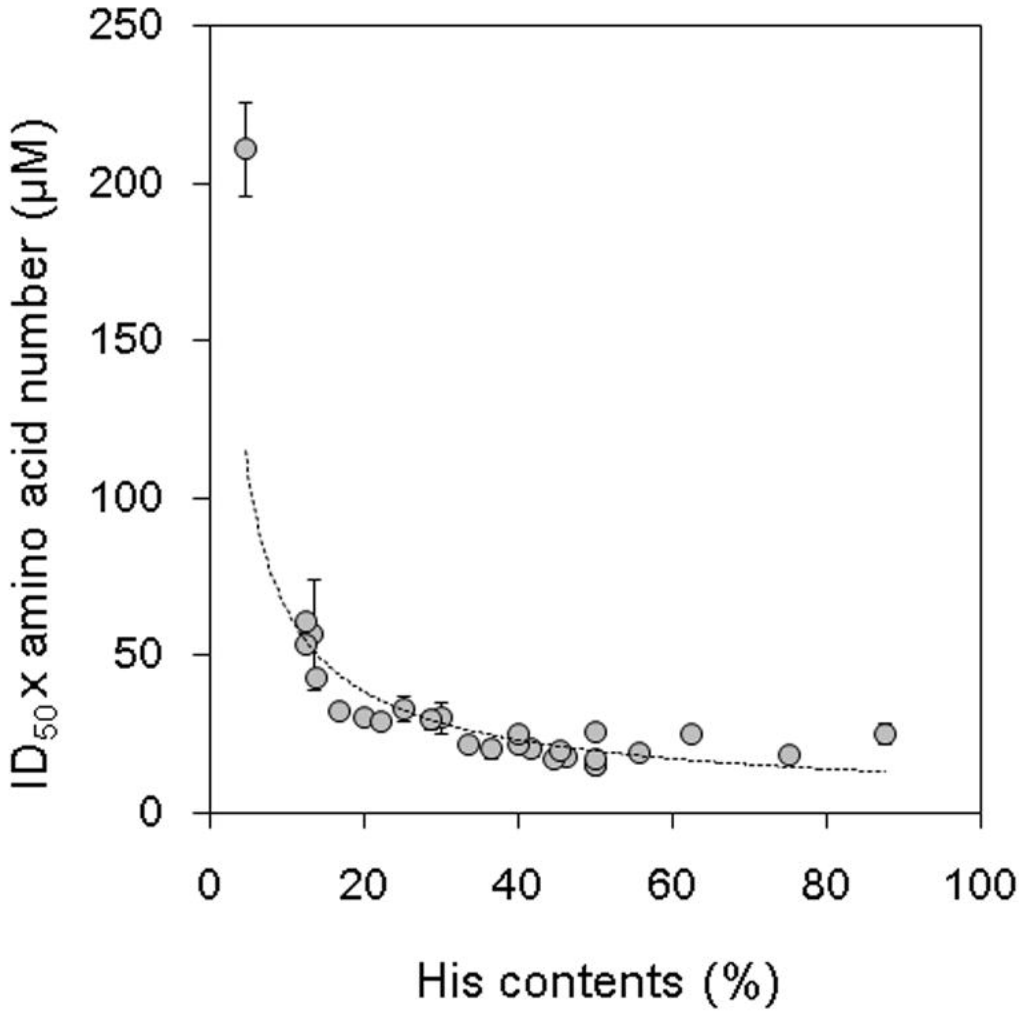

Fig. 6 Hara et al.

Title: A KS-type dehydrin and its related domains reduce Cu-promoted radical generation and the His residues contribute to the radical-reducing activities
Authors: M Hara, M Kondo, T Kato

KS dehydrins

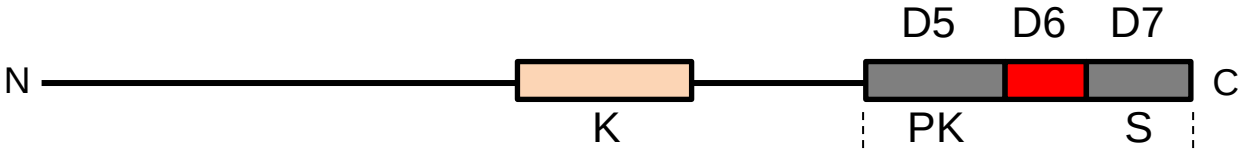

Species	Accession	Gene name			
Arabidopsis thaliana	At1g54410	*AtHIRD11*	71	EKKKKKDKKEKKHHDDGHHSSSSDSDSD	98
Oryza sativa	AAB66889		55	KEKKDKKKKEKKHGEEGHHHDGHSSSSSDSD	86
Retama raetam	AAK73280		87	EKKKKKDKKHEHGHEHGHDSSSSDSD	113
Glycine max	BAA19768	*SRC1*	76	EKKKKKDKKKKEHGHDHHGHSSSSDSD	102
Sorghum bicolor	XP_002466730		71	KEKKDKKKKEKKHGEGHDHDGHSSSSSDSD	101
Medicago sativa	AAA16927	*CAS15*	110	EKKKKKEKKKHGEGHEHGHDSSSSDSD	136
Carica papaya	AF334211		65	EEKKKKKKEKKHDEHGHDGHSSSSSSDSD	93
Brachypodium distachyon	XP_003561646		70	KEKKDKKKKKEKKHGEGHKKEDGHSSSSDSD	100
Vaccinium vitis	ACJ54952	*COR11*	83	EKKKKEKKKKHEDGHDHGGSSSSDSD	108
Corylus mandshurica	AER13139	*DHN1*	88	KKKKKDKKKHGEGHKHGDSSSSDSD	112
Ricinus communis	CAC84735	*ITP2*	74	EKKKKKKEKKKHEHGHSSSSDSD	96
Hordeum vulgare	AAT81473	*Dhn13*	73	KEKKEKKDKKKKKDKKDGEGHKDDDGHSSSSSDSD	107
Plantago major	CAH58741		83	EKKKKKKKEKKHGEGHDGGSSSSDSD	109

K_2S dehydrin

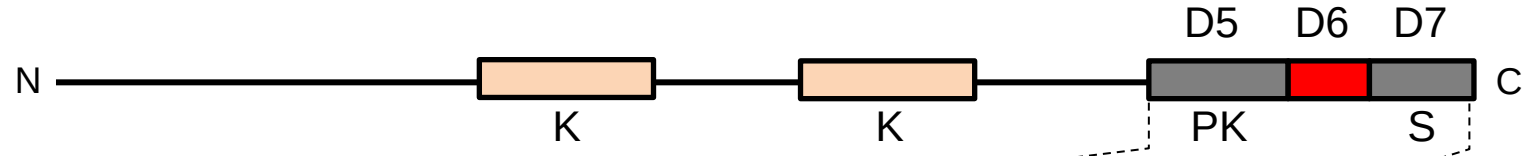

Species	Accession	Gene name			
Citrus unshiu	BAD97812	*CuCOR15*	112	EEKKKKKKEKKKHEDGHESSSSSDSD	137

Fig. S1. Amino acid sequences of D5s, D6s, and D7s in different K_nS-type dehydrins. K, PK, and S indicate K-, PK-, and S-segments, respectively. D5 and D7 are PK- and S-segments, respectively. The sequences of D6s are highlighted in red. Numbers show the positions of the sequences in the corresponding dehydrins.

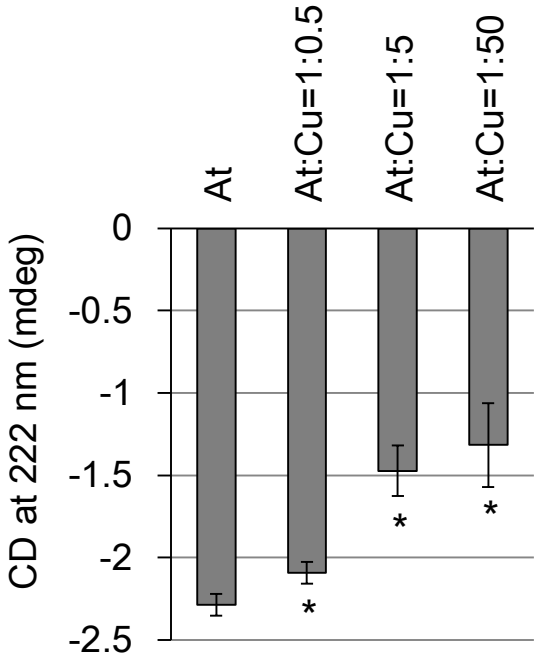

Fig. S2. Circular dichroism (CD) analyses using AtHIRD11 with different concentrations of Cu^{2+}. Difference spectrum at 222 nm between AtHIRD11 plus Cu^{2+} and Cu^{2+} alone is shown. For example, “At : Cu=1 : 0.5” means that the [AtHIRD11] : [Cu^{2+}] ratio is 1 : 0.5. “At” refers to the control without Cu^{2+}. In all cases, the AtHIRD11 concentration was 4.6 μM. Values and bars indicate means and SD of four measurements, respectively. *Significant difference ($p < 0.05$) in comparison to the “At” condition was determined by Student’s t-test.

Title: A KS-type dehydrin and its related domains reduce Cu-promoted radical generation and the His residues contribute to the radical-reducing activities
Authors: M Hara, M Kondo, T Kato

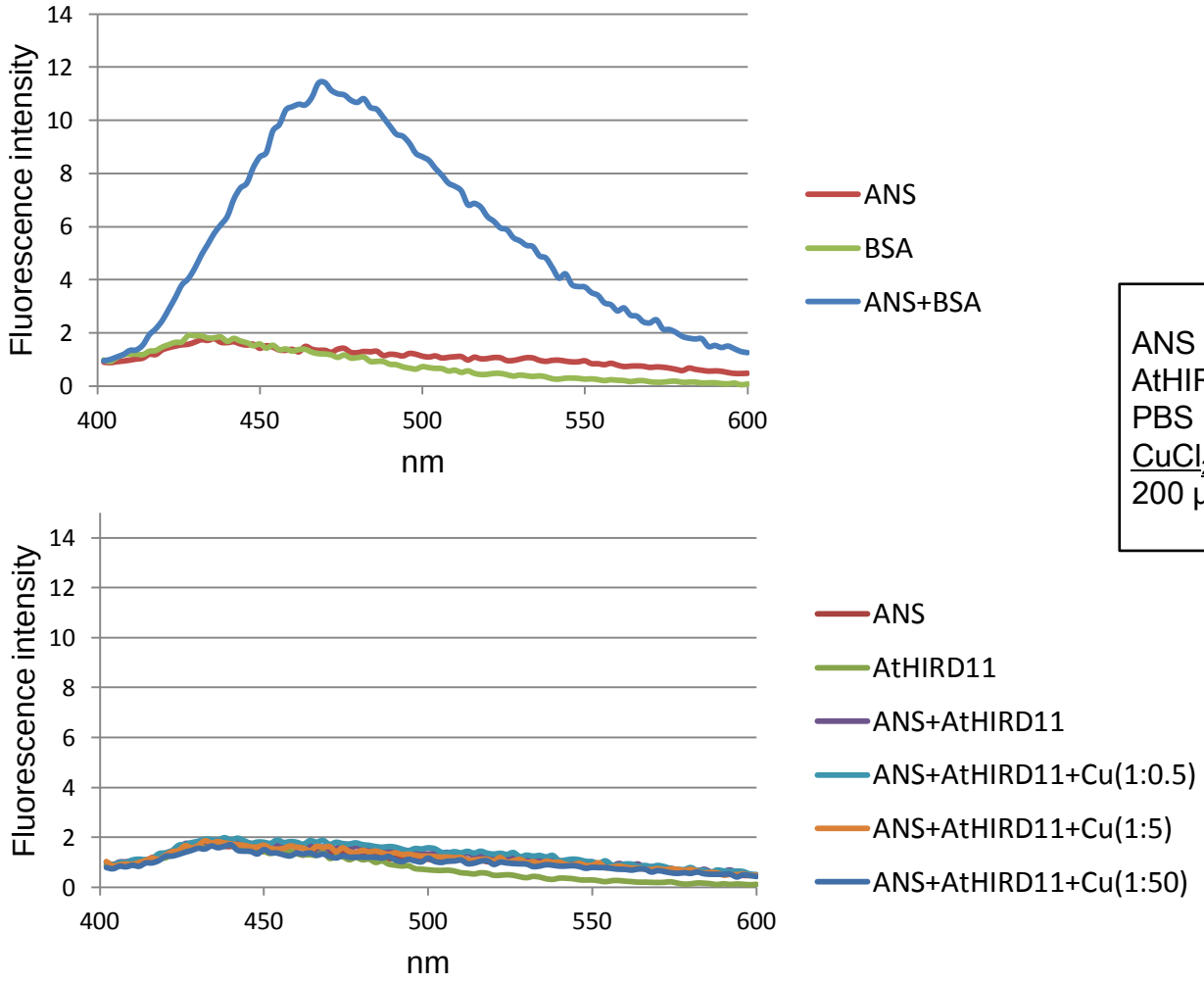

Fig. S3. AtHIRD11 did not form an ordered aggregation when Cu^{2+} was added. The ordered aggregation was detected using the 1-anilino-8-naphthalene sulfonate (ANS) assay. BSA was used as a control (the upper graph). Although BSA does not aggregate, BSA shows a positive result in the ANS assay due to its characteristic as a molten globule protein. AtHIRD11 was analyzed with or without Cu^{2+} (the lower graph). The mixture is shown at the right side of the graphs. Fluorescence (Ex 380 nm and Em 400 nm-600 nm) was measured (Thermo Scientific, Varioskan Flash microplate reader). Values were averages of 3 measurements.